Rubric 2. SCIENTIFIC AND PRACTICAL DEVELOPMENTS
Field – Electrical Engineering

DOI 10.17816/transsyst20206163-79

© A. Heya, K. Hirata, N. Niguchi
Osaka University
(Osaka, Japan)

LINEAR VERNIER ACTUATOR WITH TWO MOVERS

Background: Linear motion devices for industrial machines and robots are expected to realize their high efficiency drive and simple structure. Usually, a feed screw mechanism composed of a rotary motor and a ball-screw or slide-screw is employed. However, it has some problems such as the decrease of the drive efficiency, flexibility against external forces, noise, etc. Various linear actuators and motors have been developed utilizing the feature of a direct drive.

Aim: In this paper, we propose a novel linear actuator which 2 movers can be independently controlled using 3-phase and 6-phase superimposed currents for decreasing the size and weight of the system. The proposed linear actuator is driven by the operating principle of a vernier motor which is expected to achieve a high thrust force density per permanent magnet volume.

Methods: The operating principle and the static thrust force characteristics of the proposed linear actuator are verified by an electromagnetic field analysis using 3-D finite element method, and the back electromotive force characteristics are also analyzed. In addition, the dynamic characteristics under position feedback control are analyzed. The control system uses a vector control using PID controller, and the control input is given by the 3-phase and 6-phase superimposed currents.

Results: The static force characteristics were investigated. From the analyzed results, the force interference between the two movers was small. Moreover, the interference of the back electromotive force of the 3-phase and 6-phase movers were not observed. The movers could be independently driven under position feedback control using 3-phase and 6-phase superimposed currents. The dynamic characteristics analyses showed that the mover well followed a target position. From a step response, the time constant and the response of the position feedback system were investigated.

Conclusion: This paper presents a linear vernier actuator with two movers. The basic structure and operating principle of the actuator were described. Moreover, the static characteristics and the dynamic characteristics under position feedback control were analyzed. It was found that the movers can be independently driven.

Keywords: Linear actuator, Vernier motor, Electromagnetic actuator, 3-D FEM, Superimposed current.

Received: 28.01.2020 **Revised: 28.01.2020** **Accepted: 30.03.2020**
Поступил: 28.01.2020 **Одобрена: 28.01.2020** **Принята: 30.03.2020**

INTRODUCTION

Linear motion devices for industrial machines and robots are expected to realize their high efficiency drive and simple structure. Usually, a feed screw mechanism composed of a rotary motor and a ball-screw or slide-screw is employed. The mechanism utilizes frictional forces. Therefore, it has some problems such as the decrease of the drive efficiency, flexibility against external forces, noise, etc. In order to solve the problems, various linear actuators and motors have been developed utilizing the feature of a direct drive [1- 3]. In particular, a linear electromagnetic actuator (LEA) has many advantages such as a high drive efficiency, reduction of a noise, maintenance-free operation, and high-precision positioning.

The LEAs can drive flexibly against external forces due to a magnetic spring effect. Therefore, the LEAs are expected to apply an artificial muscle for a humanoid robot. Nakata et al. developed upper and lower extremity robots using LEAs [4]. Fujimoto et al. developed a musculoskeletal biped robot driven by LEAs [5]. These systems need a lot of linear actuators and links, and have some problems such as the increase in size and weight.

In order to solve these problems, we propose a novel linear actuator with two movers which can be independently controlled. The proposed actuator is driven by the operating principle of a vernier motor which is expected to achieve a high thrust force density per permanent magnet volume. The movers can be independently driven using 3-phase and 6-phase superimposed currents.

In this paper, the force characteristics and dynamic performance of the proposed linear actuator are investigated. The force characteristics are computed by an electromagnetic field analysis using 3-D finite element method. The dynamic characteristics under position feedback control are also verified.

LINEAR VERNIER ACTUATOR WITH TWO MOVERS

The basic structure of the proposed actuator is shown in Fig. 1 (a). The stator consists of coils, permanent magnets, and yokes. The permanent magnets and teeth are arranged at even intervals. All permanent magnets are magnetized in the y-axis direction. The winding direction are shown in Fig. (b). The movers shown in Fig. (c) consist of only a yoke. Therefore, the amount of permanent magnet does not increase. Moreover, the number of teeth of the movers is different from each other.

The operating principle is shown in Fig. 2. The proposed actuator is driven by the operational principle of a vienier motor [6]. A magnetomotive force is modulated due to a permeance distribution, and a modulated magnetic flux is generated.

Received: 28.01.2020 **Revised: 28.01.2020** **Accepted: 30.03.2020**
Поступил: 28.01.2020 **Одобрена: 28.01.2020** **Принята: 30.03.2020**

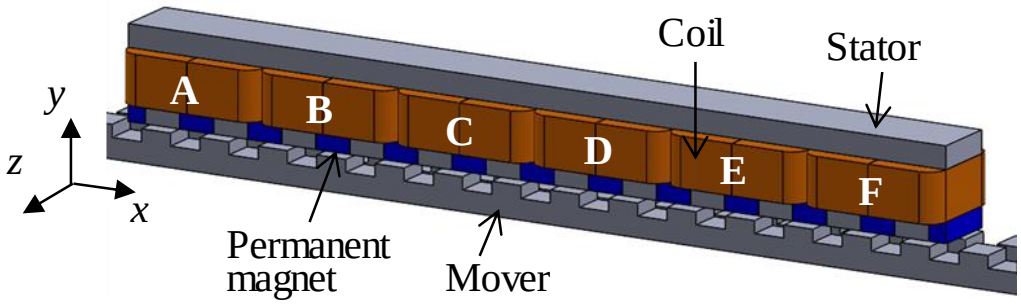

(a) Overview of the structure

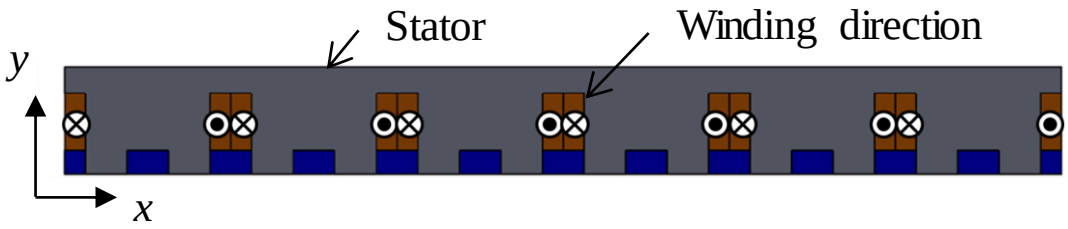

(b) Cross-sectional view of the stator

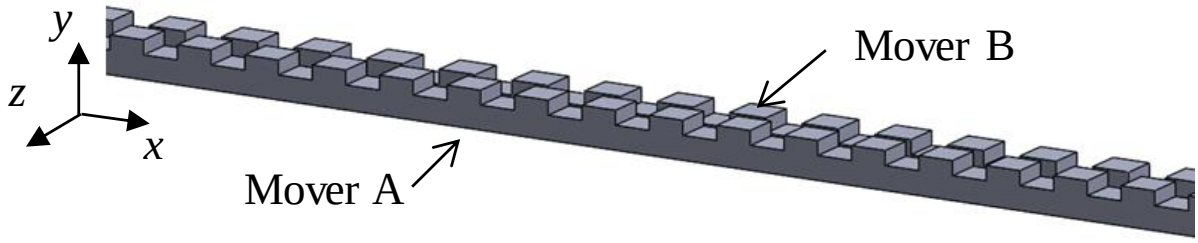

(c) Overview of the movers

Fig. 1. Basic structure of the proposed linear actuator

The magnetomotive force of the stator is defined as follows:

$$F = \sin\frac{2\pi Z_s}{L}p \tag{1}$$

where Z_s is the number of pole pairs of the stator, L is the stator length, and p is the position of the mover. The fundamental component of the mover permeance distribution is defined as follows:

$$R_p = a + \sin\frac{2\pi Z_m}{L}p \tag{2}$$

where Z_m is the number of pole pairs of the mover, and a is the average permeance of the mover. The modulated magnetic flux in the air gap is defined as follows:

Received: 28.01.2020 Revised: 28.01.2020 Accepted: 30.03.2020
Поступил: 28.01.2020 Одобрена: 28.01.2020 Принята: 30.03.2020

$$\varphi = F \cdot R_p = a\sin\frac{2\pi Z_s}{L}p - \frac{1}{2}\cos(Z_s + Z_m)\frac{2\pi}{L}p + \frac{1}{2}\cos(Z_s - Z_m)\frac{2\pi}{L}p \quad (3)$$

The proposed actuator is driven by synchronizing a moving magnetic field generated by the coils with a modulated magnetic flux. Therefore, the relationship of the number of teeth and order of the moving magnetic field generated by the coils is defined as follows:

$$\begin{cases} Z_s + Z_m = \pm O_c \\ Z_s - Z_m = \pm O_c \end{cases} \quad (4)$$

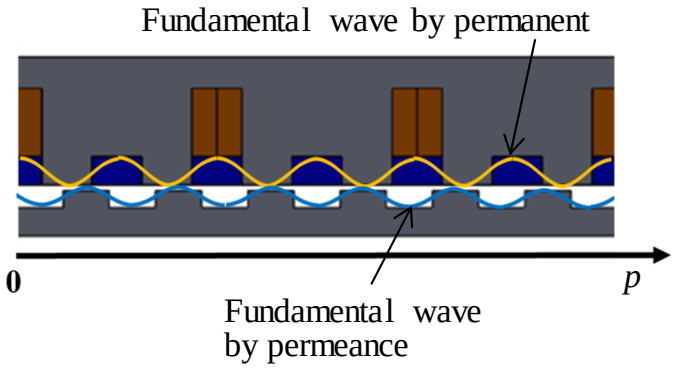

Fig. 2. Operating principle of the proposed linear actuator

where O_c is the order of the moving magnetic field generated by the coils.

The armature current of the proposed actuator has 3-phase and 6-phase alternating currents (ACs), and each mover utilizes either of them to move. The 3-phase AC is defined as follows:

$$\begin{cases} I_U = \sqrt{2}I\sin\left(\frac{2\pi Z_1 p_1}{L}\right) \\ I_V = \sqrt{2}I\sin\left(\frac{2\pi Z_1 p_1}{L} - \frac{2\pi}{3}\right) \\ I_W = \sqrt{2}I\sin\left(\frac{2\pi Z_1 p_1}{L} - \frac{4\pi}{3}\right) \end{cases} \quad (5)$$

where Z_1 and p_1 is the number of salient pole pairs and position of the mover driven by the 3-phase AC, respectively, and I is the effective current. Similarly, The 6-phase AC is defined as follows:

Received: 28.01.2020 Revised: 28.01.2020 Accepted: 30.03.2020
Поступил: 28.01.2020 Одобрена: 28.01.2020 Принята: 30.03.2020

$$\begin{cases} I_A = \sqrt{2}I\sin\left(\frac{2\pi Z_2 p_2}{L}\right) \\ I_B = \sqrt{2}I\sin\left(\frac{2\pi Z_2 p_2}{L} - \frac{\pi}{3}\right) \\ I_C = \sqrt{2}I\sin\left(\frac{2\pi Z_2 p_2}{L} - \frac{2\pi}{3}\right) \\ I_D = \sqrt{2}I\sin\left(\frac{2\pi Z_2 p_2}{L} - \pi\right) \\ I_E = \sqrt{2}I\sin\left(\frac{2\pi Z_2 p_2}{L} - \frac{4\pi}{3}\right) \\ I_F = \sqrt{2}I\sin\left(\frac{2\pi Z_2 p_2}{L} - \frac{5\pi}{3}\right) \end{cases} \quad (6)$$

where Z_2 and p_2 is the number of salient pole pairs and position of the mover driven by the 6-phase AC, respectively. The interlinkage flux of the 3-phase coils is defined as follows:

$$\begin{cases} \phi_U = \phi\cos\left(\frac{2\pi Z_1 p_1}{L}\right) \\ \phi_V = \phi\cos\left(\frac{2\pi Z_1 p_1}{L} - \frac{2\pi}{3}\right) \\ \phi_W = \phi\cos\left(\frac{2\pi Z_1 p_1}{L} - \frac{4\pi}{3}\right) \end{cases} \quad (5)$$

where Φ is the amplitude of the interlinkage flux. Simiraly, the interlinkage flux of the 6-phase coils is defined as follows:

$$\begin{cases} \phi_A = \phi\cos\left(\frac{2\pi Z_2 p_2}{L}\right) \\ \phi_B = \phi\cos\left(\frac{2\pi Z_2 p_2}{L} - \frac{\pi}{3}\right) \\ \phi_C = \phi\cos\left(\frac{2\pi Z_2 p_2}{L} - \frac{2\pi}{3}\right) \\ \phi_D = \phi\cos\left(\frac{2\pi Z_2 p_2}{L} - \pi\right) \\ \phi_E = \phi\cos\left(\frac{2\pi Z_2 p_2}{L} - \frac{4\pi}{3}\right) \\ \phi_F = \phi\cos\left(\frac{2\pi Z_2 p_2}{L} - \frac{5\pi}{3}\right) \end{cases} \quad (6)$$

The force of the mover due to the 6-phase magnetic flux and 3-phase AC is defined as follows:

$$F_{36} = I_U\phi_A + I_V\phi_B + I_W\phi_C + I_U\phi_D + I_V\phi_E + I_W\phi_F = 0 \quad (7)$$

The force of the mover due to the 3-phase magnetic flux and 6-phase AC is defined as follows:

Received: 28.01.2020 Revised: 28.01.2020 Accepted: 30.03.2020
Поступил: 28.01.2020 Одобрена: 28.01.2020 Принята: 30.03.2020

$$F_{63} = I_A\phi_U + I_B\phi_V + I_c\phi_W + I_D\phi_U + I_E\phi_V + I_F\phi_W = 0 \quad (8)$$

From (7) and (8), the interference of the force is zero. Thus, the movers can be independently driven [7, 8].

The proposed actuator is controlled using vector control, and 3-phase and 6-phase ACs are transformed into d-q axis. The transformation matrix of the currents from the UVW to d-q coordinate systems is defined as follows:

$$\begin{bmatrix} I_{d3} \\ I_{q3} \end{bmatrix} = D_3 \begin{bmatrix} I_U \\ I_V \\ I_W \end{bmatrix} \quad (9)$$

$$D_3 = \sqrt{\frac{2}{3}} \begin{bmatrix} \cos\theta & \cos(\theta - \frac{2}{3}\pi) & \cos(\theta - \frac{4}{3}\pi) \\ -\sin\theta & -\sin(\theta - \frac{2}{3}\pi) & \sin(\theta - \frac{4}{3}\pi) \end{bmatrix} \quad (10)$$

where θ is the electrical angle of the position defined as follows:

$$\theta = \frac{2\pi Zp}{L} \quad (11)$$

where Z is the number of salient pole pairs of the mover. The transformation matrix of the currents from the ABCDEF to dq coordinate systems is defined as follows:

$$\begin{bmatrix} I_{d6} \\ I_{q6} \end{bmatrix} = D_6 \begin{bmatrix} I_A \\ I_B \\ I_C \\ I_D \\ I_E \\ I_F \end{bmatrix} \quad (12)$$

$$D_6 = \sqrt{\frac{1}{3}} \begin{bmatrix} \cos\theta & \cos(\theta - \frac{1}{3}\pi) & \cos(\theta - \frac{2}{3}\pi) & \cos(\theta - \pi) & \cos(\theta - \frac{4}{3}\pi) & \cos(\theta - \frac{5}{3}\pi) \\ -\sin\theta & -\sin(\theta - \frac{1}{3}\pi) & -\sin(\theta - \frac{2}{3}\pi) & -\sin(\theta - \pi) & -\sin(\theta - \frac{4}{3}\pi) & -\sin(\theta - \frac{5}{3}\pi) \end{bmatrix} \quad (13)$$

The inverse d-q transformation of the voltage from dq to UVW coordinate systems is defined as follows:

Received: 28.01.2020 Revised: 28.01.2020 Accepted: 30.03.2020
Поступил: 28.01.2020 Одобрена: 28.01.2020 Принята: 30.03.2020

$$\begin{bmatrix} V_U \\ V_V \\ V_W \end{bmatrix} = {D_3}^{-1} \begin{bmatrix} V_{d3} \\ V_{q3} \end{bmatrix} \tag{14}$$

$${D_3}^{-1} = \sqrt{\frac{2}{3}} \begin{bmatrix} \cos\theta & -\sin\theta \\ \cos(\theta - \frac{2}{3}\pi) & -\sin(\theta - \frac{2}{3}\pi) \\ \cos(\theta - \frac{4}{3}\pi) & -\sin(\theta - \frac{4}{3}\pi) \end{bmatrix} \tag{15}$$

The inverse d-q transformation of the voltage from dq to ABCDEF coordinate systems is defined as follows:

$$\begin{bmatrix} V_A \\ V_B \\ V_C \\ V_D \\ V_E \\ V_F \end{bmatrix} = {D_6}^{-1} \begin{bmatrix} V_{d6} \\ V_{q6} \end{bmatrix} \tag{16}$$

$${D_6}^{-1} = \sqrt{\frac{1}{3}} \begin{bmatrix} \cos\theta & -\sin\theta \\ \cos\left(\theta - \frac{1}{3}\pi\right) & -\sin\left(\theta - \frac{1}{3}\pi\right) \\ \cos\left(\theta - \frac{2}{3}\pi\right) & -\sin\left(\theta - \frac{2}{3}\pi\right) \\ \cos(\theta - \pi) & -\sin(\theta - \pi) \\ \cos\left(\theta - \frac{4}{3}\pi\right) & -\sin\left(\theta - \frac{4}{3}\pi\right) \\ \cos\left(\theta - \frac{5}{3}\pi\right) & -\sin\left(\theta - \frac{5}{3}\pi\right) \end{bmatrix} \tag{17}$$

The block diagram of the control system is shown in Fig. 3. In this paper, $I_d = 0$ control is used. The position feedback control is achieved using a PID control. A PI control is used for the current control. The 3-phase AC is extracted from the superimposed current as follows:

Received: 28.01.2020 **Revised: 28.01.2020** **Accepted: 30.03.2020**
Поступил: 28.01.2020 **Одобрена: 28.01.2020** **Принята: 30.03.2020**

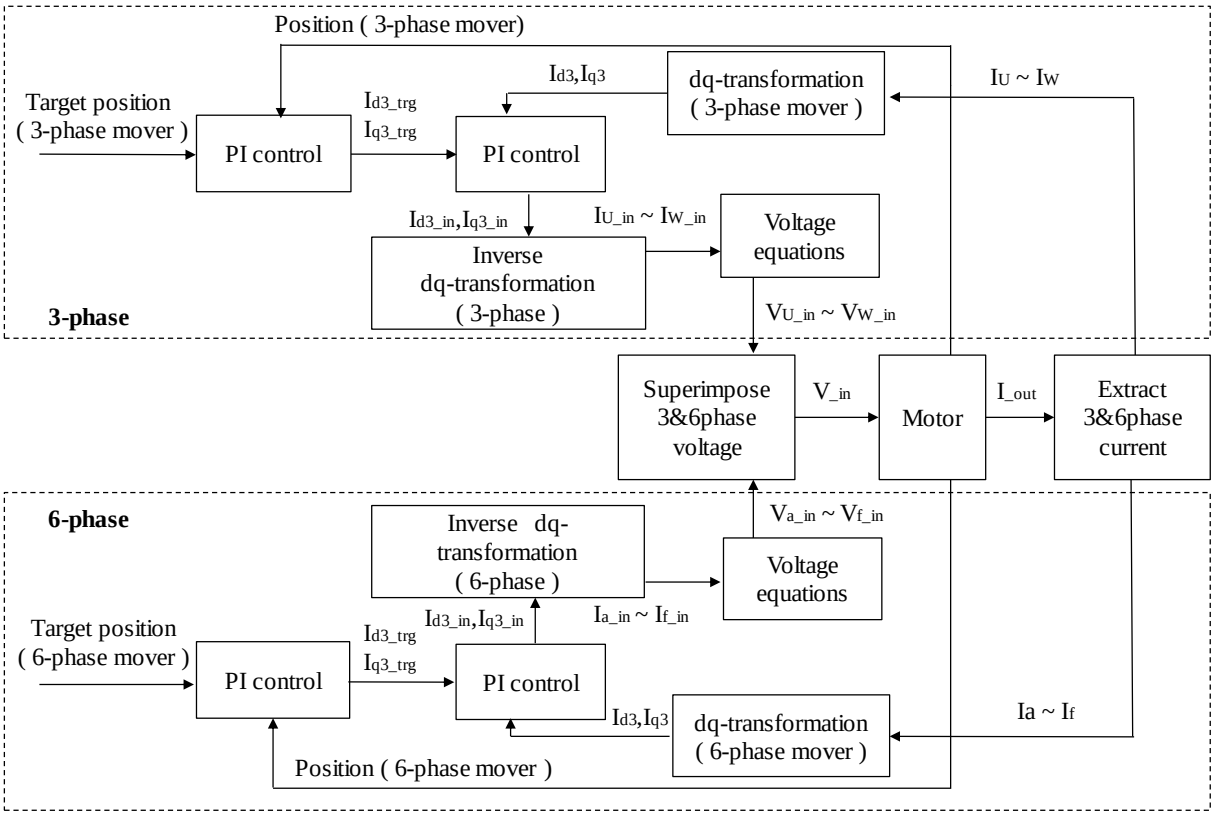

Fig. 3. Block diagram of the control system

$$\begin{cases} I_a = I_A + I_U \\ I_b = I_B + I_V \\ I_c = I_C + I_W \\ I_d = I_D + I_U \\ I_e = I_E + I_V \\ I_f = I_F + I_W \end{cases} \quad (18)$$

From (18), the 3-phase AC is defined as follows:

$$\begin{cases} I_U = \frac{I_a + I_d - (I_A + I_D)}{2} \\ I_V = \frac{I_a + I_d - (I_A + I_D)}{2} \\ I_W = \frac{I_a + I_d - (I_A + I_D)}{2} \end{cases} \quad (19)$$

The relationship of the 6-phase ACs is defined as follows:

$$\begin{cases} I_A + I_D = 0 \\ I_B + I_E = 0 \\ I_C + I_F = 0 \end{cases} \quad (20)$$

Received: 28.01.2020 **Revised: 28.01.2020** **Accepted: 30.03.2020**
Поступил: 28.01.2020 **Одобрена: 28.01.2020** **Принята: 30.03.2020**

From (19) and (20), the component of the 3-phase AC can be extracted. The 6-phase AC is extracted from the superimposed current as follows:

$$\begin{cases} I_A = I_a - I_U \\ I_B = I_b - I_V \\ I_C = I_c - I_W \\ I_D = I_d - I_U \\ I_E = I_e - I_V \\ I_F = I_f - I_W \end{cases} \quad (21)$$

From (19), the component of the 6-phase AC can also be extracted.

RESULTS OF CHARACTERISTICS ANALYSIS

The specification of the analysis model is shown in Table 1. The dimensions of the stator and mover are shown in Tables 2 and 3. The length of one period of the 3-phase and 6-phase movers is 15 mm and 16.15 mm, respectively. The positional relationship of the movers and stator is shown in Fig. 4.

Table 1. Specification of the analysis model

Number of coils	6
Number of pole pairs of the stator	12
Air gap length [mm]	1
Residual magnetic flux density [Br]	1.4
Distance between movers [mm]	1.5
Number of coil turns	388
Coil space factor [%]	63
Maximum amplitude of current [A]	0.6

Table 2. Dimensions of the movers

	3-phase	6-phase
Fundamental order of permeance	14	13
Total height [mm]	8	8
Pole height [mm]	3	3
Pole width [mm]	7.5	8.08

Table 3. Dimensions of the movers

Height [mm]	22.5
Width [mm]	210
Depth [mm]	16
Back yoke height [mm]	5.5
Permanent magnet height [mm]	5
Permanent magnet width [mm]	8.75
Permanent magnet depth [mm]	16

Received: 28.01.2020 **Revised: 28.01.2020** **Accepted: 30.03.2020**
Поступил: 28.01.2020 **Одобрена: 28.01.2020** **Принята: 30.03.2020**

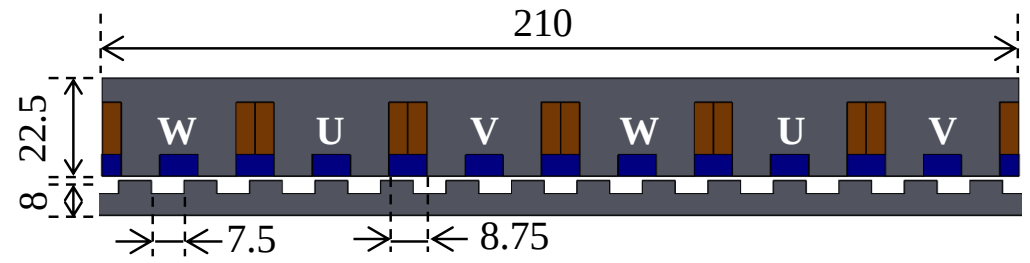

(a) 3-phase mover

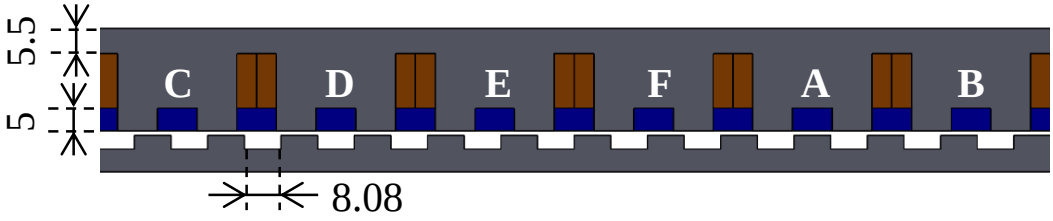

(b) 6-phase mover

Fig. 4. Positional relationship of the movers and stator

For verifying the static force characteristics, a 3-D finite element method is used [9, 10]. The 3-D mesh model except for the air region is shown in Fig. 5. The analysis conditions are shown in Table 4. In the static force analysis, the amplitude of the 3-phase and 6-phase ACs is 0.6 A. The current density is 5 A/mm^2.

The analysis patterns are defined as follows:

Pattern 1-1: The 3-phase mover is moved under 3-phase AC, and the 6-phase mover is fixed.

Pattern 1-2: The 6-phase mover is moved under 6-phase AC, and the 3-phase mover is fixed.

Pattern 1-3: Both movers are moved under 3-phase and 6-phase superimposed currents.

The static force analysis results of each pattern are shown in Figs. 6, 7, and 8. The average forces are shown in Table 4. From the results of pattern 1-1, the average force of the 3-phase and 6-phase movers is 6.47 N and 0.24 N, respectively. It is found that the 3-phase mover can be driven by the 3-phase AC. From the results of pattern 1-2, the average force of the 3-phase and 6-phase movers is 0.007 N and 5.70 N, respectively. It shows that the 6-phase mover can be driven by the 6-phase AC. From the results of pattern 1-3, the average force of the 3-phase and 6-phase movers is 5.89 N and 5.13 N, respectively. It is observed that the 3-phase and 6-phase movers can be driven by only the 3-phase and 6-phase AC, respectively.

Received: 28.01.2020 **Revised: 28.01.2020** **Accepted: 30.03.2020**
Поступил: 28.01.2020 **Одобрена: 28.01.2020** **Принята: 30.03.2020**

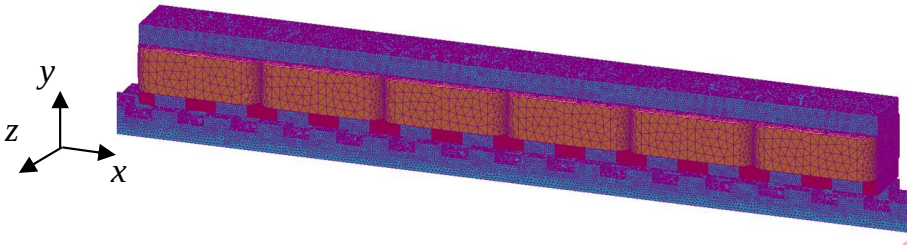

Fig. 5. 3-D mesh model except for the air region

Table 4. Analysis conditions

Number of elements	4,730,229
Number of nodes	801,229
Number of edges	5,532,118
CPU time [h]	12.5

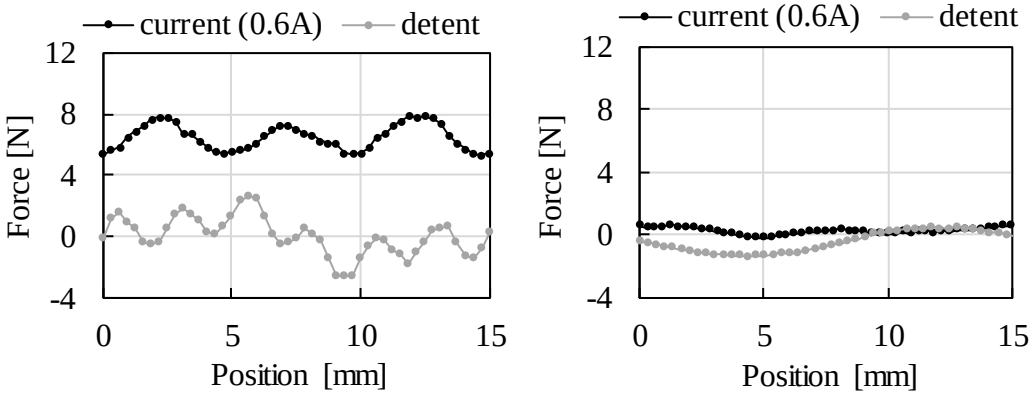

Fig. 6. Analysis results of the force characteristics (Pattern 1-1)

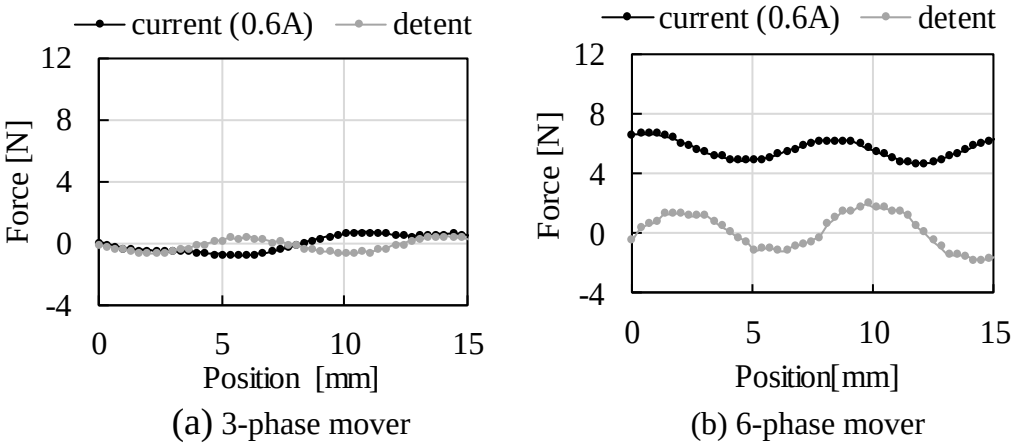

Fig. 7. Analysis results of the force characteristics (Pattern 1-2)

Received: 28.01.2020
Поступил: 28.01.2020
Revised: 28.01.2020
Одобрена: 28.01.2020
Accepted: 30.03.2020
Принята: 30.03.2020

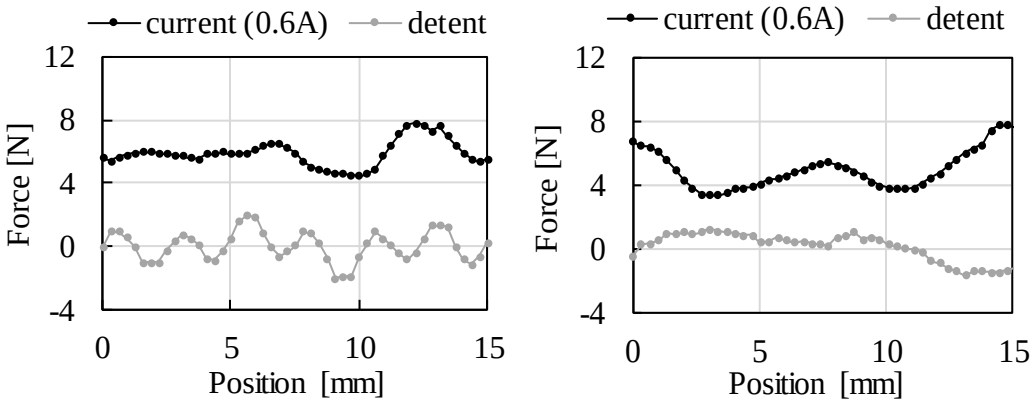

Fig. 8. Analysis results of the force characteristics (Pattern 1-3)

Table 4. Average force of the proposed linear actuator

	Average force of the 3-phase mover [N]	Average force of the 6-phase mover [N]
Pattern 1	6.47	0.24
Pattern 2	0.007	5.70
Pattern 3	5.89	5.13

For verifying the independency of both movers, the back electromotive force is analyzed. In this study, the analysis patterns are shown as follows:

Pattern 2-1: Only the 3-phase mover is moved.

Pattern 2-2: Only the 6-phase mover is moved.

Pattern 2-3: Both movers are moved

The moving velocity is 300 mm/s, and the operating time is 100 ms.

The analysis results are shown in Fig. 9. From these results, the back electromotive force of pattern 2-3 is the composition of that of pattern 1 and pattern 2. It shows that the movers can be independently driven.

For verifying the dynamic performance under position feedback control, the dynamic characteristics analysis is conducted. The target trajectory is given using a trapezoidal velocity waveform. The analysis patterns using the target trajectory are shown as follows:

Pattern 3-1: The 3-phase mover is controlled for the target trajectory, and the 6-phase mover is controlled to be fixed.

Pattern 3-2: The 6-phase mover is controlled for the target trajectory, and the 3-phase mover is controlled to be fixed.

Pattern 3-3: Both movers are controlled for the target trajectory

The target trajectory is shown in Fig. 10. The maximum velocity and acceleration is 0.4 m/s and 0.2 m/s^2, respectively The PID controller gain is shown in Table 5. In this control, the control period is 2.5 ms. The mass of each mover is 3 kg.

Received: 28.01.2020 **Revised: 28.01.2020** **Accepted: 30.03.2020**
Поступил: 28.01.2020 **Одобрена: 28.01.2020** **Принята: 30.03.2020**

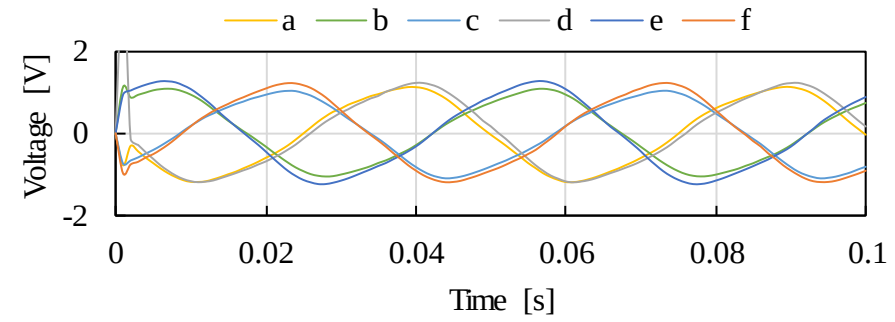

(a) Pattern 2-1

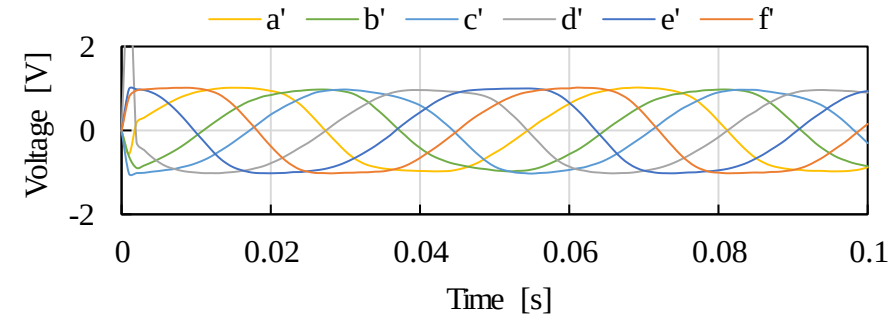

(b) Pattern 2-2

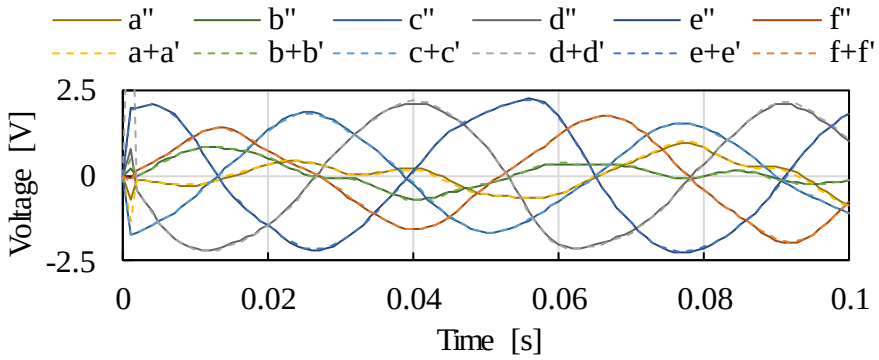

(c) Pattern 2-3

Fig. 9. Analysis results of the back electromotive force

Table 5. PID controller gain

		Current controller	Position controller
3-phase	*Kp*	4.85	300
	Ki	0.24	10
	Kd	-	150
6-phase	*Kp*	4.85	300
	Ki	0.24	10
	Kd	-	150

The computed dynamic characteristics are shown in Figs. 11, 12, and 13. From the results, the steady-state error is very small, and both movers can be controlled following the target trajectory.

Received: 28.01.2020 **Revised: 28.01.2020** **Accepted: 30.03.2020**
Поступил: 28.01.2020 **Одобрена: 28.01.2020** **Принята: 30.03.2020**

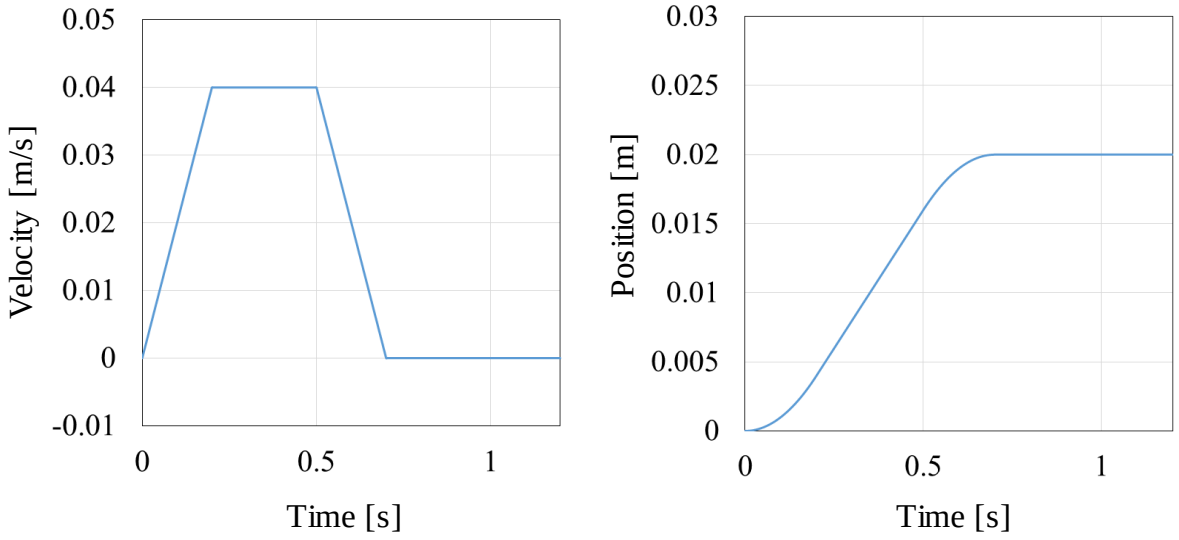

(a) Velocity trajectory (b) Position trajectory

Fig. 10. Target trajectory

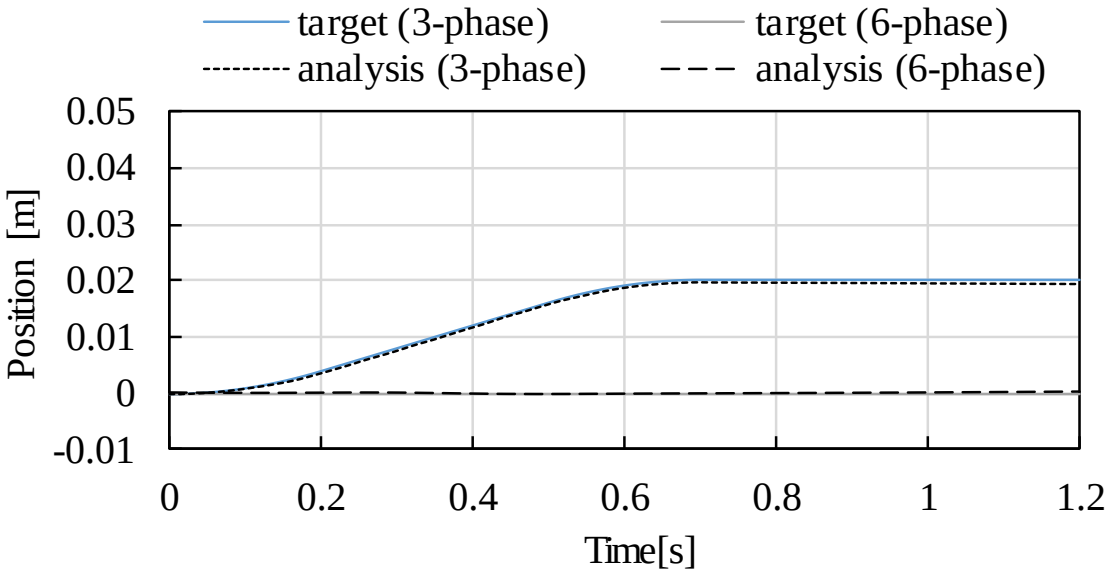

Fig. 11. Analysis results of the position feedback control (Pattern 3-1)

Received: 28.01.2020
Поступил: 28.01.2020
Revised: 28.01.2020
Одобрена: 28.01.2020
Accepted: 30.03.2020
Принята: 30.03.2020

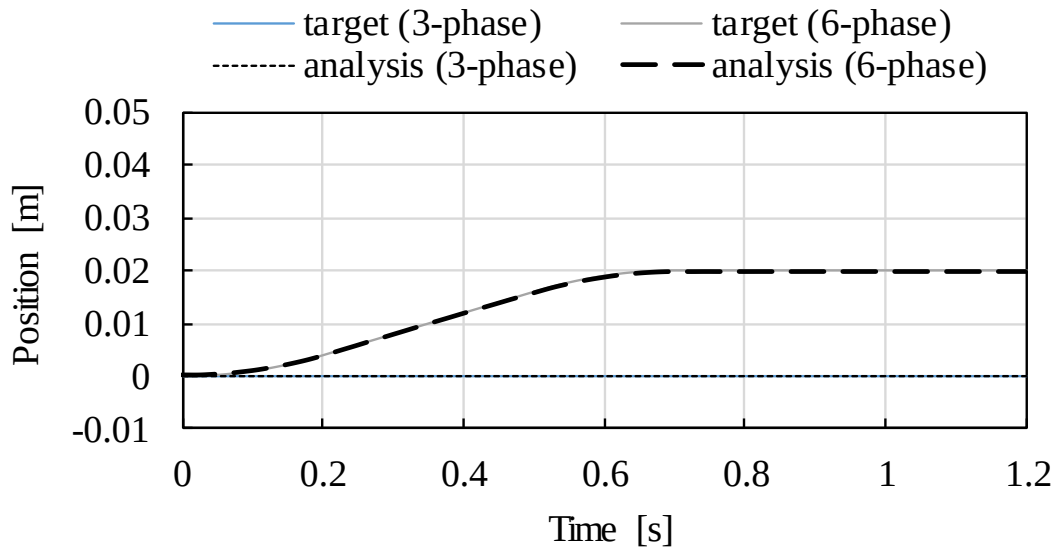

Fig. 12. Analysis results of the position feedback control (Pattern 3-2)

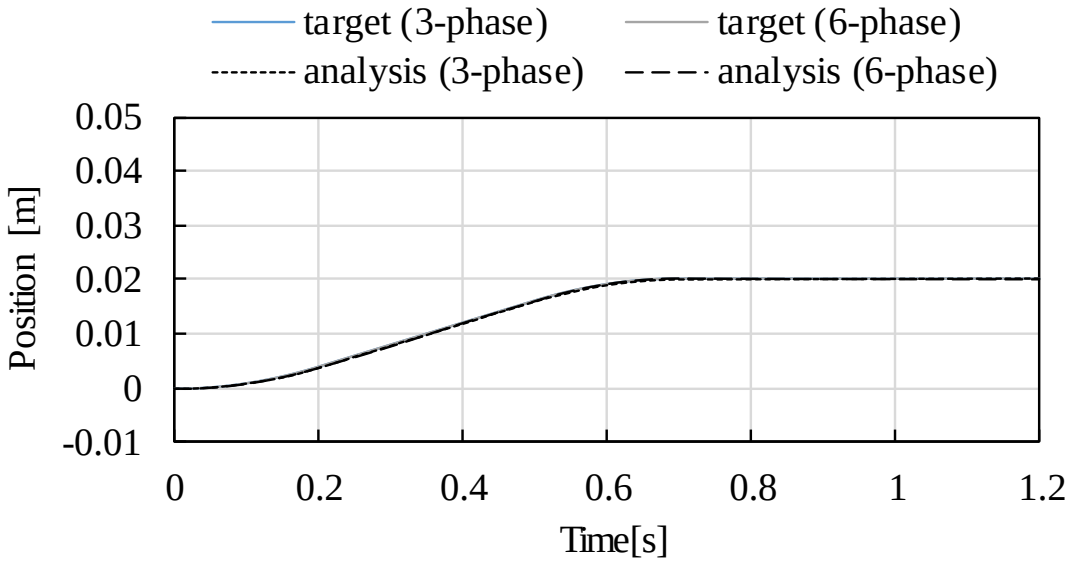

Fig. 13. Analysis results of the position feedback control (Pattern 3-3)

The step response of the control system is also analyzed. The analysis patterns are shown as follows:

Pattern 4-1: The step target trajectory is applied to the 3-phase mover, and the 6-phase mover is controlled to be fixed.

Pattern 4-2: The step target trajectory is applied to the 6-phase mover, and the 3-phase mover is controlled to be fixed.

The analysis results of the step response are shown in Fig. 14. The time constant of the mover of the 3-phase and 6-phase movers is 0.115 s and 0.125 s, respectively. From the results, the mover well followed the target trajectory, and the movers can be independently controlled.

Received: 28.01.2020 **Revised: 28.01.2020** **Accepted: 30.03.2020**
Поступил: 28.01.2020 **Одобрена: 28.01.2020** **Принята: 30.03.2020**

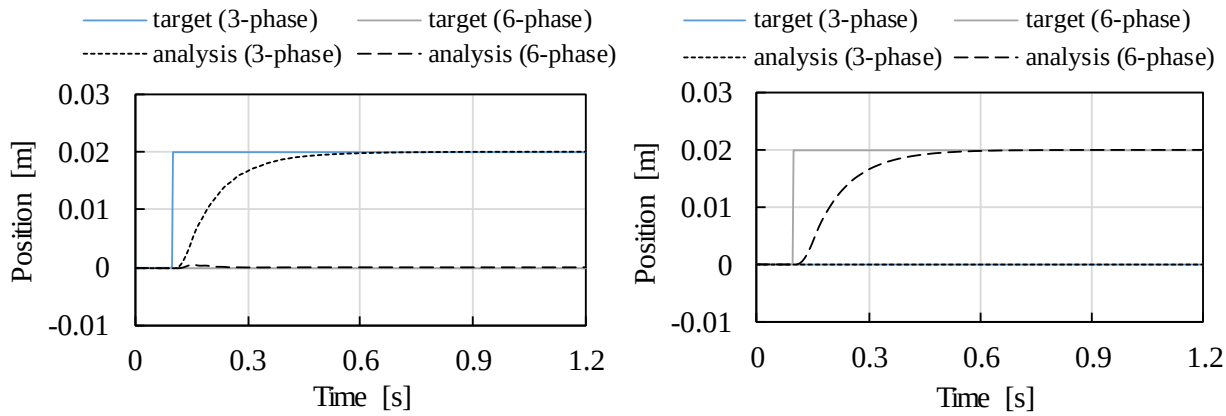

(a) Pattern 4-1 (b) Pattern4-2

Fig. 14. Analysis results of the step response

CONCLUSION

In this paper, we proposed a linear vernier actuator with two movers. The basic structure, the operating principle, and the control method of the two movers were described. The force characteristics were investigated by the magnetic field analysis using 3-D finite element method. The dynamic characteristics under position feedback control were verified, and it was found that the movers can be independently controlled. In future works, we will verify the control performance on a prototype.

References

1. Niu S, Ho SL, Fu WN. Performance Analysis of a Novel Magnetic Geard Tubular Linear Permanent Magnetic Machine. *IEEE Trans. Magn.* 2011;47(10):3598-3601. doi.org/10.1109/tmag.2011.2148167
2. Na B, Choi H, Kong K. Design of a Direct-Driven Linear Actuator for a High-Speed Quadruped Robot, Cheetaroid-I. *IEEE/ASME Trans. Mechatron*. 2015;20(2):924-933. doi: 10.1109/tmech.2014.2326696
3. Zheng LL, Yao BY, Wang Q. Desired Compensation Adaptive Robust Control of a Linear-Motor-Driven Precision Industrial Gantry With Improved Cogging Force Compensation. *IEEE/ASME Trans. Mechatron*. 2008;13(6):617-624. doi: 10.1109/tmech.2008.2003510
4. Nakata Y, Hiroshi H, Hirata K. Dynamic Analysis Method for Electromagnetic Artificial Muscle Actuator under PID Control. *IEEE Trans. Ind. Appl.* 2011;131(2):166-170. doi: 10.1541/ieejias.131.166
5. Fujimoto Y, Kominami T, Hamada H. Development and Analysis of a High Thrust Force Direct-Drive Linear Actuator. *IEEE Trans. On Ind. Elec.* 2009;56(5):1383-1392. doi: 10.1109/tie.2009.2012419
6. Toba A, Lipo TA. Generic Torque Maximizing Design Methodology of Surface Permanent Magnet Vernier Machine. *IEEE Trans. Ind. Appl.* 2000;36(6):1539-1546. doi: 10.1109/28.887204

Received: 28.01.2020 **Revised: 28.01.2020** **Accepted: 30.03.2020**
Поступил: 28.01.2020 **Одобрена: 28.01.2020** **Принята: 30.03.2020**

7. Kohara A, Hirata K, Niguchi N, Ohno Y. Finite-Element Analysis and Experiment of Current Superimposition Variable Flux Machine Using Permanent Magnet. 2016;52(9)8107807. doi: 10.1109/tmag.2016.2572659
8. Suzuki H, Hirata K, Niguchi N, Kohara A. Characteristics Verification of a Novel Motor with Two Controllable Rotors. In Proc. *IEEE Int. Magn. Conf*. 2018; EG-10:898. doi: 10.1109/intmag.2018.8508233
9. Webb JP, Forghani B. A T-Ω method using hierarchal edge elements. *in Proc. IEE, Sci. Meas. Technol*. 1995;142(2):133-141. doi: 10.1049/ip-smt:19951439
10. Webb JP, Forghani B. DC Current Distributions and Magnetic Fields using the T-Ω Edge-Element Method. *IEEE Trans. Mgn.* 1995;31(3):1444-1447. doi: 10.1109/20.376300

Information about the authors:

Akira Heya, Ph.D. Student, Yamadaoka, Suita, Osaka 565-0871, Japan
ORCID: 0000-0001-5966-4387;
E-mail: Akira.heya@ams.eng.osaka-u.ac.jp

Katsuhiro Hirata, Professor,
ORCID: 0000-0002-5597-5265;
E-mail: k-hirata@ams.eng.osaka-u.ac.jp

Noboru Niguchi, Assistant professor,
ORCID: 0000-0002-1005-7946;
E-mail: noboru.niguchi@ams.eng.osaka-u.ac.jp

To cite this article:

Heya A, Hirata K, Niguchi N. Linear Vernier Actuator with Two Movers. *Transportation Systems and Technology*. 2020;6(1):63-79. doi: 10.17816/transsyst20206163-79

Received: 28.01.2020 **Revised: 28.01.2020** **Accepted: 30.03.2020**
Поступил: 28.01.2020 **Одобрена: 28.01.2020** **Принята: 30.03.2020**